Computational Modeling and Analysis For Complex Systems
NSF Expedition in Computing

CMACS: AFIB Challenge

Radu Grosu

Stony Brook University

http://cmacs4heart.pbworks.com/

2nd Year Review Meeting, Carnegie Mellon University

November 3, 2011

Team So Far:
CMACS Atrial-Fibrillation

James Glimm
Stony Brook

Scott Smolka
Stony Brook

Radu Grosu
Stony Brook

Ezio Bartocci
Stony Brook

Abhishek Murthy
Stony Brook

Ariful Islam
Stony Brook

Klaus Havelund
NASA

Gerard Holzmann
NASA

Impossible Without An Expeditions Project

Robert Gilmour
Cornell

Flavio Fenton
Cornell

Elizabeth Cherry
Cornell

Oded Maler
Verimag

Gregory Batt
Inria

Nancy Griffeth
CUNY

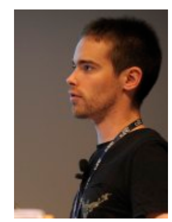

Colas Le Guernic
NYU

Patrick Cousot
NYU

Goals:
AFIB-Challenge

Model, Predict and Control Cardiac Arrhythmias

In particular Atrial and Ventricular Fibrillation

Extend developed tools and techniques for the

Other CMACS Challenges and for any Hybrid System

Results:
CMACS-AFIB

CMACS Specific Results

- **1st GPU-based 2D and 3D simulation** of all important human cardiac models
- **1st automatic parameter-range identification** for abnormal behavior in cardiac cells
- **1st GPU-based curvature analysis and classification** of abnormal cardiac behavior
- **1st Low energy defibrillation** of atrial and ventricular tissue in vitro and in vivo

Cross-Cutting Fundamental Results

- **An optimal linearization algorithm** of for nonlinear experimental data signals
- **GPU-techniques for real-time simulation** of nonlinear partial-differential equations
- **Robust verification and PR identification** for MHA and time-dependent properties
- **Distributed control algorithms** for nonlinear systems with stiff PDE
- **Optimal model repair techniques** for discrete- and continuous-time Markov Chains
- **Techniques for checking ε-bisimulation** among continuous-time MDPs
- **Development of a time-frequency logic** to better capture signal properties
- **Improve time-space performance** of verification tools with GPU-Mutlicore techniques

Motivation:
AFIB-Challenge

Normal Heart Beat

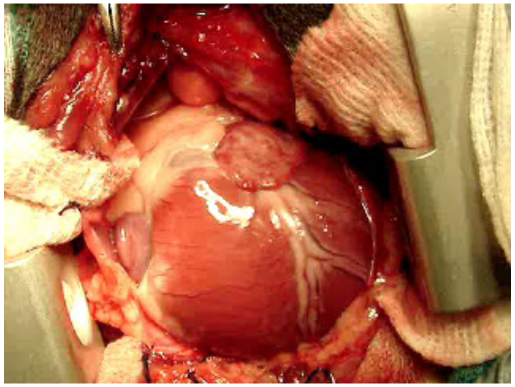

Atrial Fibrillation

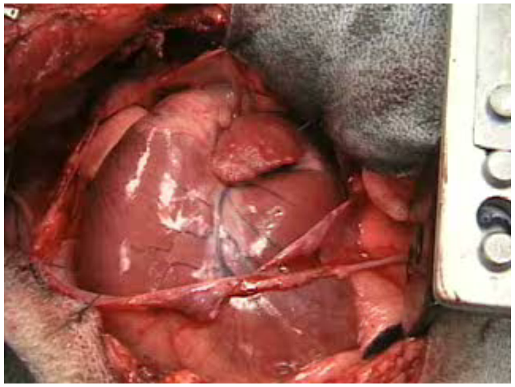

Heart disease is one of the leading causes of death in the world.

Ranks number one in industrialized countries.

In the USA alone:

- **1/3 of total deaths are due to heart disease.**
- **1 in 5 people have some form of heart disease.**
- **4.5 million do not die but are hospitalized every year.**
- **Economic impact: $214 billion a year.**

Motivation:
CDC / Statistics

National Vital Statistics Report, Vol.49, No.11, October 12, 2006
Deaths and percent of total deaths for the 10 leading causes of death: United States

Rank	Cause of death	Total Deaths	Percentage
	All causes	2,391,399	100.0
1	**Diseases of heart**	**725,192**	**30.3**
2	Malignant neoplasms	549,838	23.0
3	Cerebrovascular diseases	167,366	7.0
4	Chronic lower respiratory diseases	124,181	5.2
5	Accidents (unintentional injuries)	97,860	4.1
6	Diabetes mellitus	68,399	2.9
7	Influenza and pneumonia	63,730	2.7
8	Alzheimer’s disease	44,536	1.9
9	Nephritis, nephrotic syndrome and nephrosis	35,525	1.5
10	Septicemia	30,680	1.3
	All other causes	484,092	20.2

http://www.cdc.gov/nchs/data/nvsr/nvsr57/nvsr57_14.pdf

Background:
Types of Arrhythmias

- **Arrhytmias occur in upper chambers (atria) or lower chambers (ventricles) or both**
- **Heart rate may be increased or decreased**
- **May result from pacemaker dysfunction or breakdown of electrical activity (reentry)**
- **Some arrhymias are of genetic nature**
- **Arrhytmias may be asymptomatic or they may be immediately life-threatening**

Background:
Problems Studying AFIB

Complicated structure

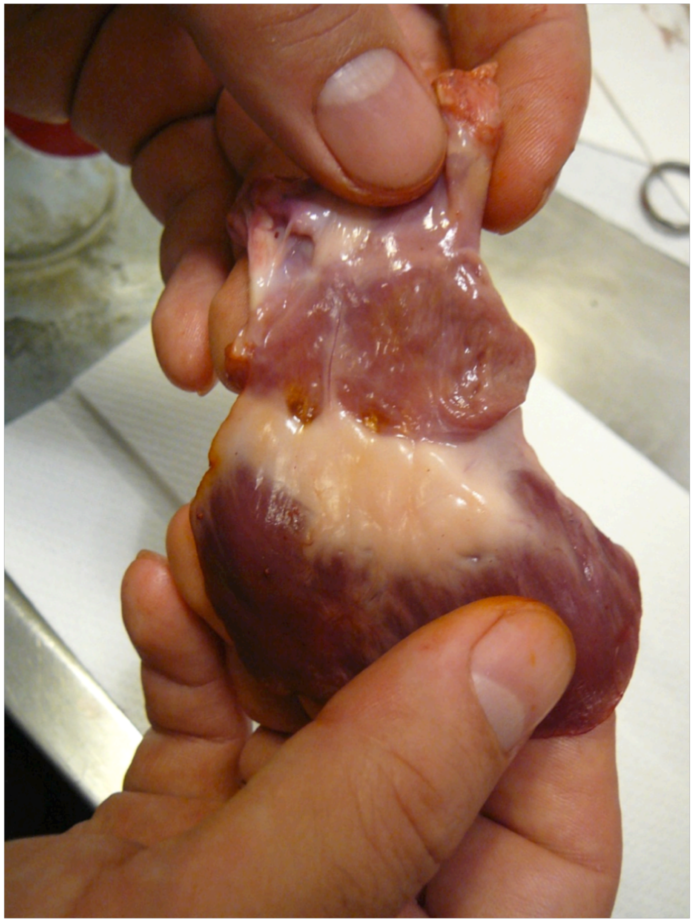

Canine heart (MRI @120 microns resolution)

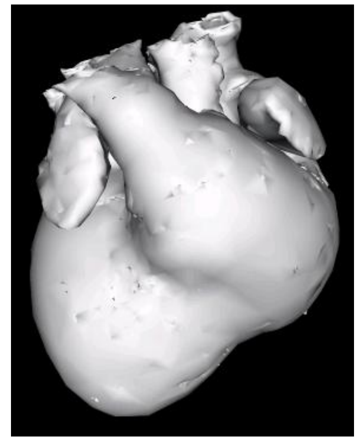

Canine heart (DTMRI @ 250 microns resolution)

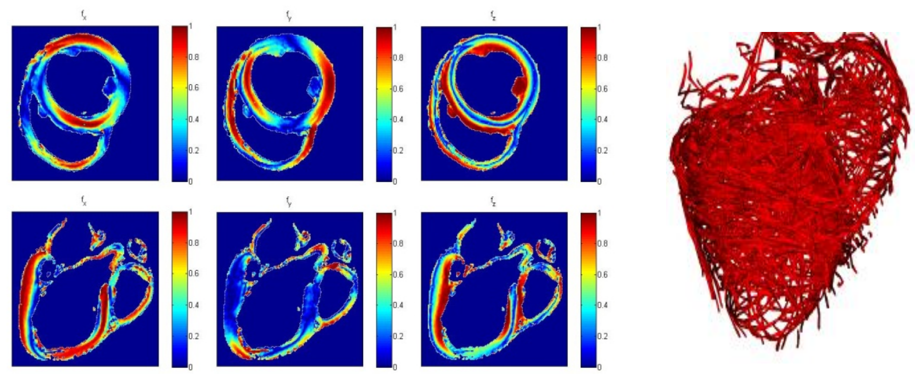

Pittsburgh NMR Center for Biomedical Research

Background:
From Experiment to Model

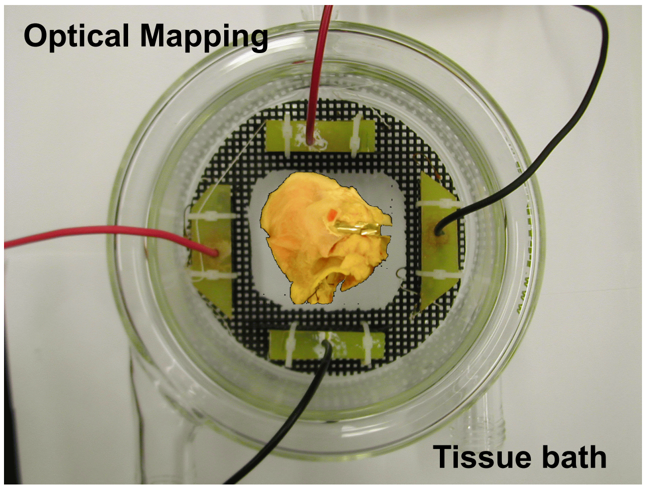

- Di-4-ANEPPS (voltage sensitive dye)
- Diodes 530 nm wavelength
- Cascade cameras at 511 Hz
- 128x128 window view

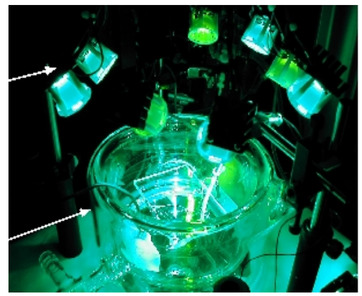

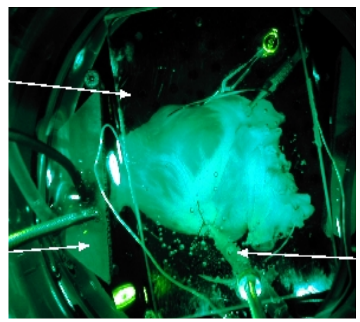

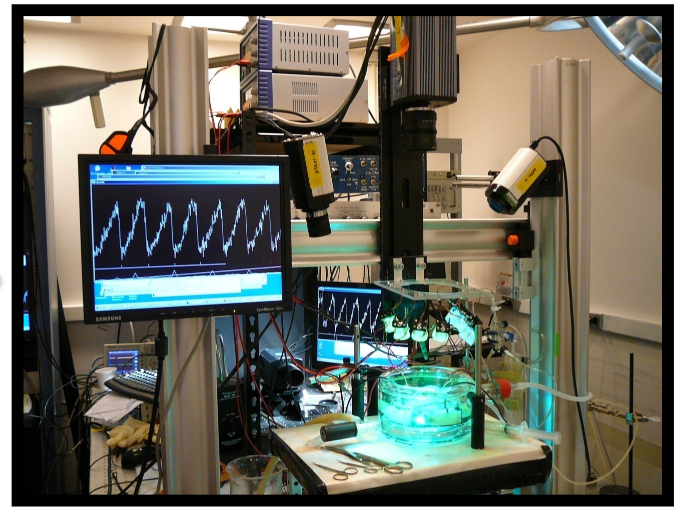

Assumption on the Form of the Model

(Non)linear Identification Of the Parameters

Microelectrode recordings

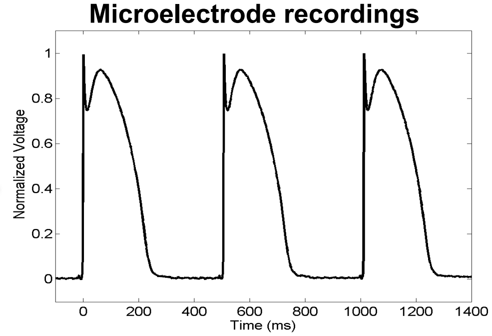

Optical mapping

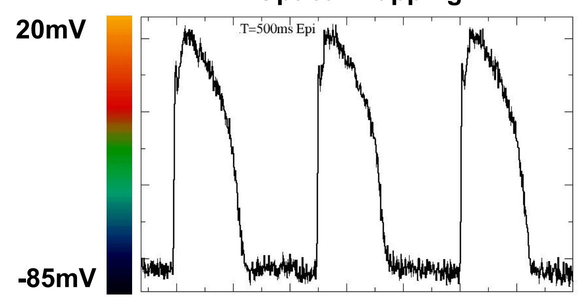

Better signal/noise
Discontinuous in space
Not for long times

Modeling: Towers of Abstraction for Analysis of Cardiac Abnormalities

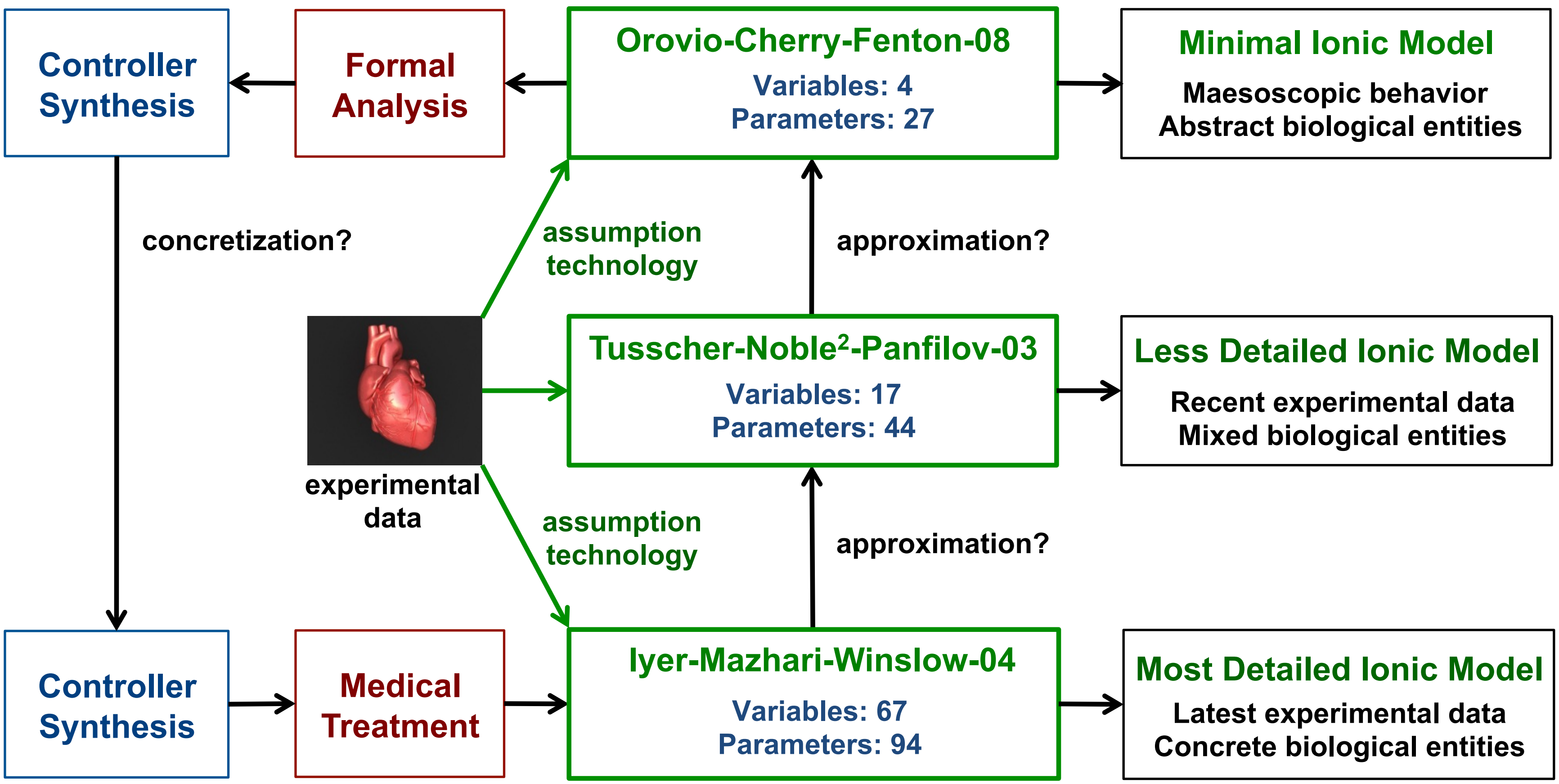

Modeling: From MM Hybrid Automaton to the Multi-Affine Hybrid Automaton

Minimal Model as a Nonlinear Hybrid Automaton

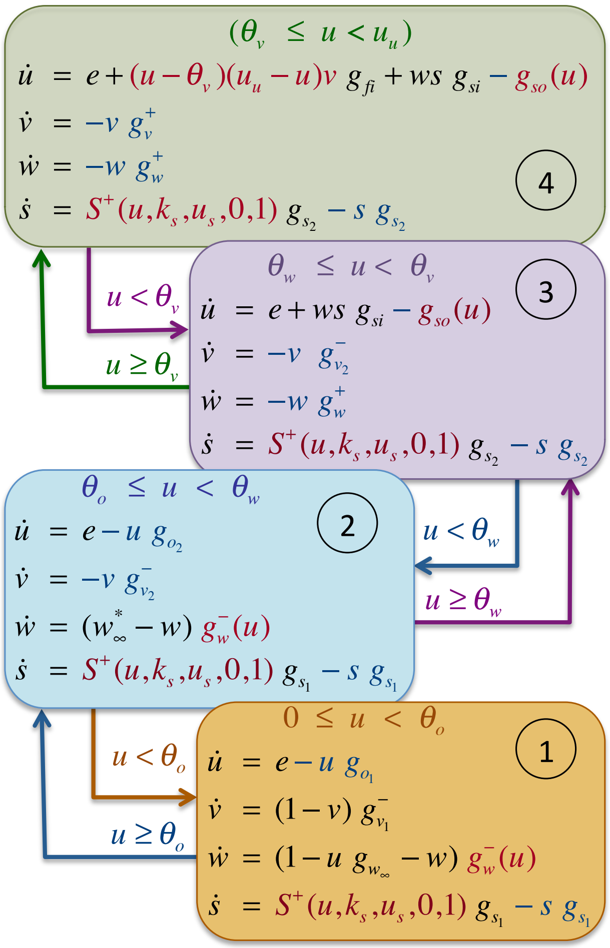

2D and 3D Simulation of Partial Differential Equations

$$\dot{u} = \nabla(D\nabla u) - (J_{fi} + J_{si} + J_{so})$$

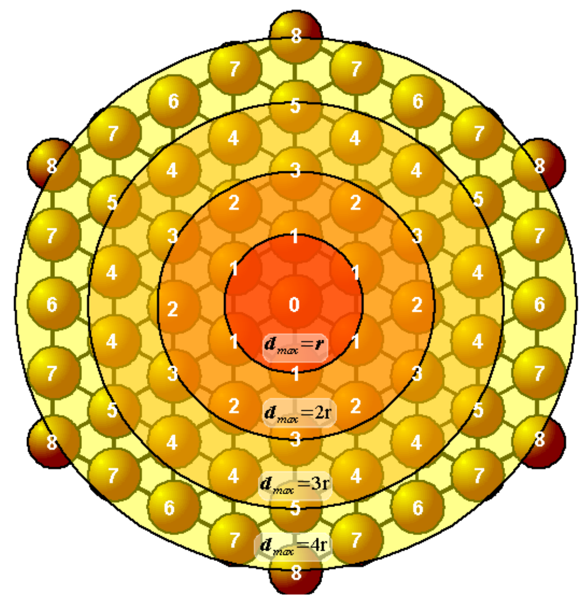

PDEs are simulated as Finite Difference Equations

Modeling: From MM Hybrid Automaton to the Multi-Affine Hybrid Automaton

Minimal Model as a Nonlinear Hybrid Automaton | **Optimal Linearization of Nonlinear Terms**

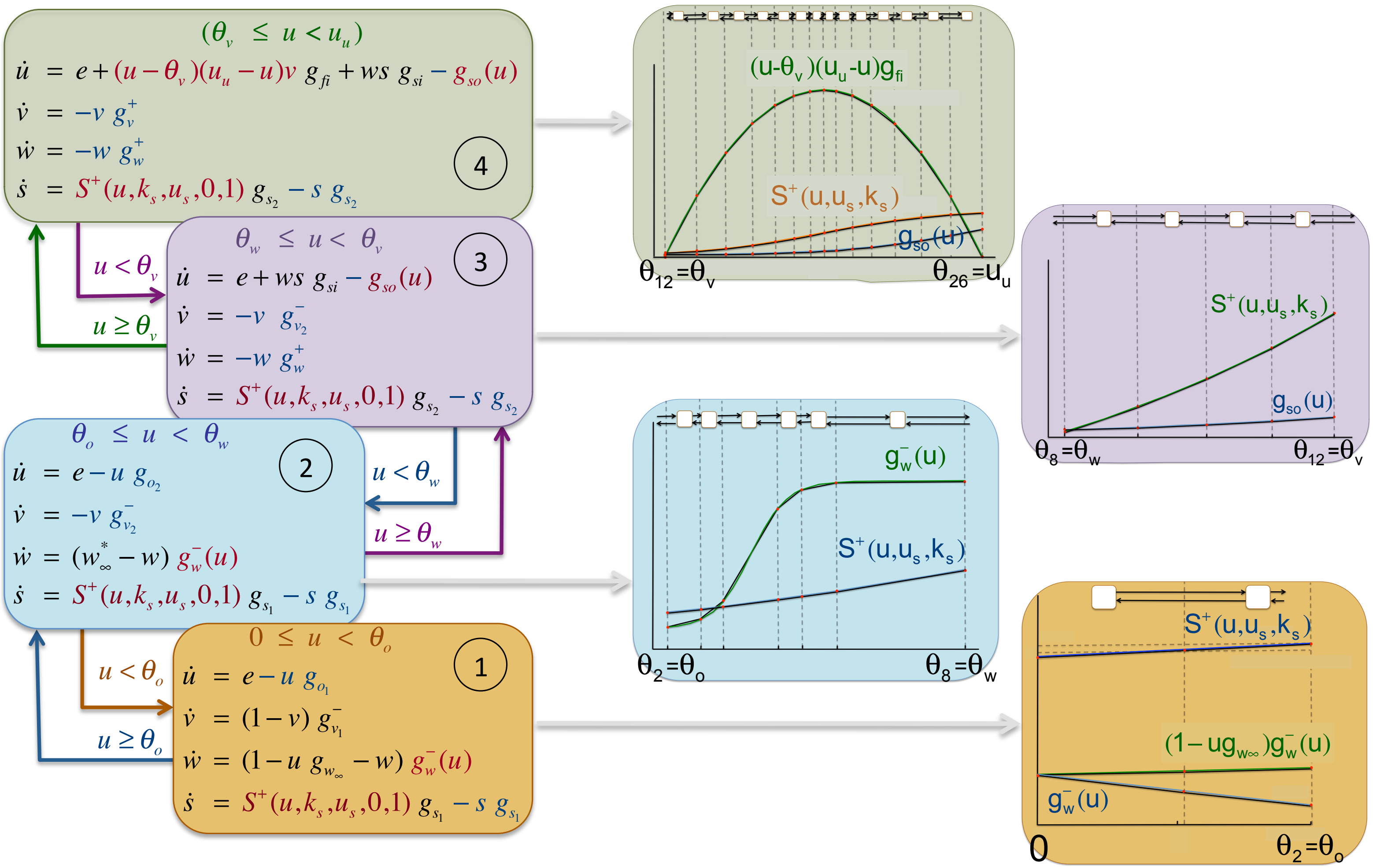

Modeling: From MM Hybrid Automaton to the Multi-Affine Hybrid Automaton

The Multi-Affine Hybrid Automaton

Mode 4: $\theta_{12} = \theta_v < u \le u_u = \theta_{26}$

$$\begin{aligned}
\dot{u} &= e + \sum_{i=12}^{25} R(u,\theta_i,\theta_{i+1},u_{fi_i},u_{fi_{i+1}})\, v\, g_{fi} + ws\, g_{si} - \sum_{i=12}^{25} R(u,\theta_i,\theta_{i+1},u_{so_i},u_{so_{i+1}})\, g_{so}\\
\dot{v} &= -v\, g_v^+\\
\dot{w} &= -w\, g_w^+\\
\dot{s} &= (\sum_{i=12}^{25} R(u,\theta_i,\theta_{i+1},u_{s_i},u_{s_{i+1}}) - s)\, g_{s_2}
\end{aligned}$$

Mode 3: $\theta_8 = \theta_w \le u < \theta_v = \theta_{12}$

$$\begin{aligned}
\dot{u} &= e + ws\, g_{si} - \sum_{i=8}^{11} R(u,\theta_i,\theta_{i+1},u_{so_i},u_{so_{i+1}})\, g_{so}\\
\dot{v} &= -v\, g_{v_2}^-\\
\dot{w} &= -w\, g_w^+\\
\dot{s} &= (\sum_{i=8}^{11} R(u,\theta_i,\theta_{i+1},u_{s_i},u_{s_{i+1}}) - s)\, g_{s_2}
\end{aligned}$$

Mode 2: $\theta_2 = \theta_o \le u < \theta_w = \theta_8$

$$\begin{aligned}
\dot{u} &= e - u\, g_{o_2}\\
\dot{v} &= -v\, g_{v_2}^-\\
\dot{w} &= (w_\infty^* - w)\, g_w^-\\
\dot{s} &= (\sum_{i=2}^{7} R(u,\theta_i,\theta_{i+1},u_{s_i},u_{s_{i+1}}) - s)\, g_{s_1}
\end{aligned}$$

Mode 1: $\theta_0 = 0 \le u < \theta_o = \theta_2$

$$\begin{aligned}
\dot{u} &= e - u\, g_{o_1}\\
\dot{v} &= (1 - v)\, g_{v_1}^-\\
\dot{w} &= (1 - u g_{w_\infty} - w)\, g_w^-\\
\dot{s} &= (\sum_{i=0}^{1} R(u,\theta_i,\theta_{i+1},u_{s_i},u_{s_{i+1}}) - s)\, g_{s_1}
\end{aligned}$$

Transitions:
- 1 → 2: $u \ge \theta_o$; 2 → 1: $u < \theta_o$
- 2 → 3: $u \ge \theta_w$; 3 → 2: $u < \theta_w$
- 3 → 4: $u \ge \theta_v$; 4 → 3: $u < \theta_v$

Comparison in 1D

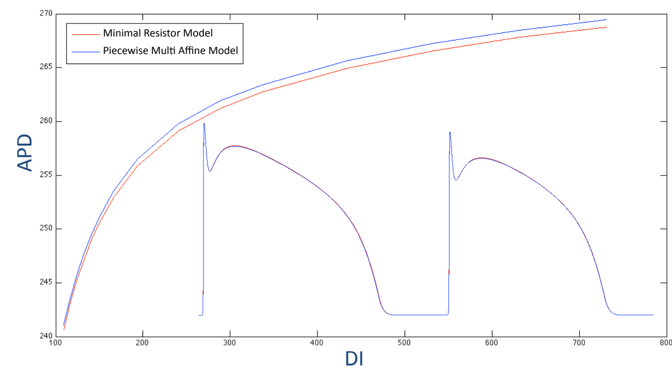

Comparison in 2D

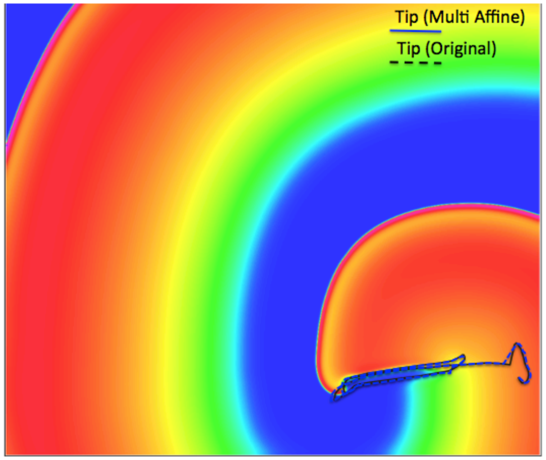

These results appeared this year in CAV'11, LNCS 6806, pp. 396-411, 2011

Modeling: Approximating the Sodium Current of the Iyer Model

Iyer's Parametric CTMC for the Sodium Channel

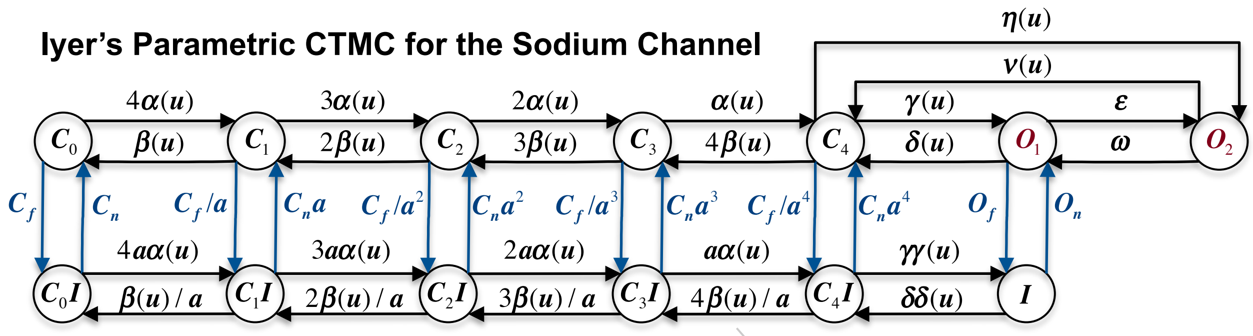

$o(t) = O_1(t) + O_2(t)$

$\alpha(u), \beta(u) \doteq ce^{au+b}$

Assuming Independence of the units

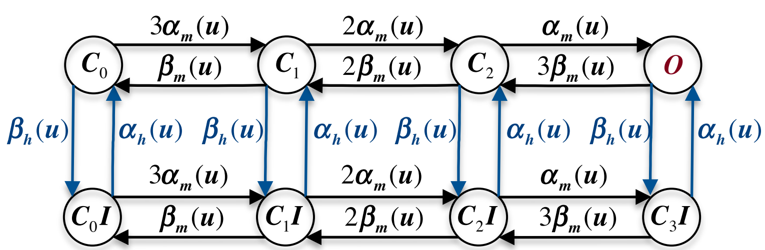

$o(t) = O(t)$

Using Stable-Invariant Manifold Reduction

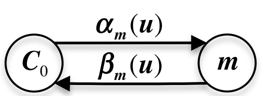

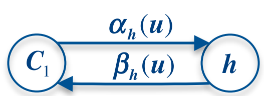

$\dot{m} = \alpha_m(u)(1-m) - \beta_m(u)m$

$\dot{h} = \alpha_h(u)(1-h) - \beta_h(u)h$

$o(t) = m(t)^3 h(t)$

Hodgkin-Huxley I_{Na} Channel

Independence between activation -inactivation

Least-Squares (Neldar-Mead) fitting, randomized seeding

Invariant Manifold Reduction

Multinomial distribution is an exact solution for 8-state parametric CTMC.

Proving ε-bisimilarity
Is work in progress

The Sodium Channel

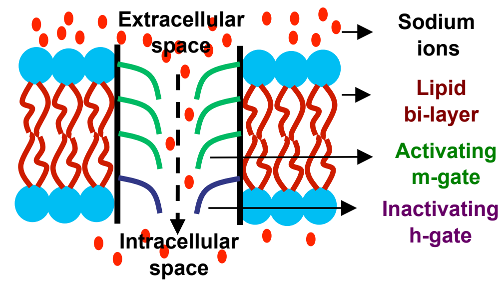

Action Potential Results

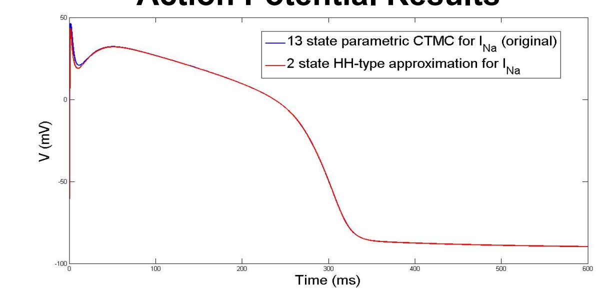

Sodium Currents in Upstroke Results

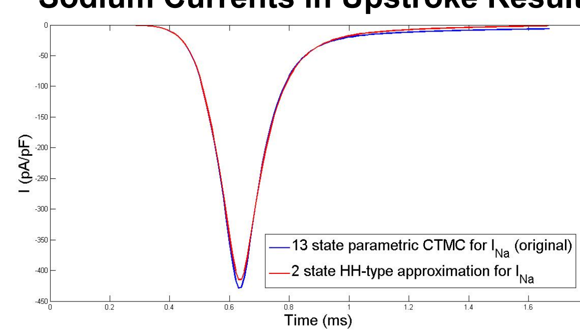

Analysis: Real Time Simulation with NVIDIA Graphical Processing Units

Minimal Model in Four State Variables (4V)

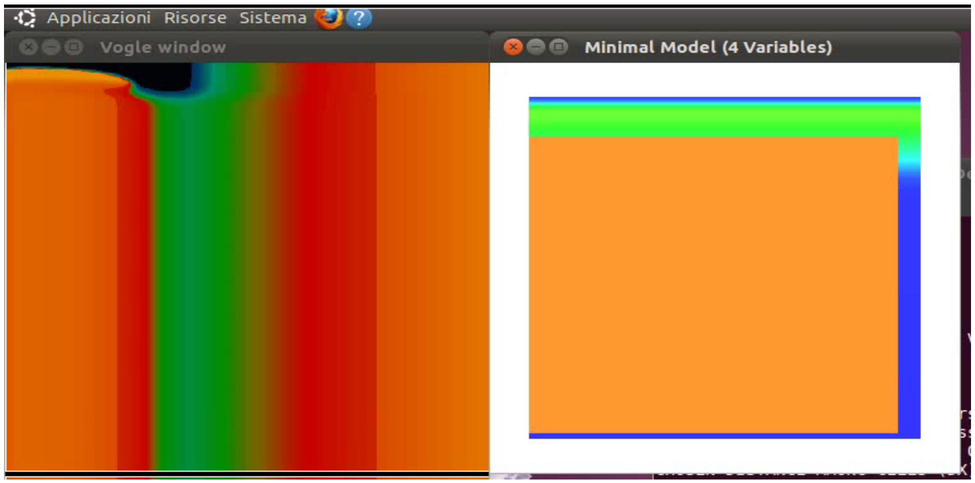

Beeler-Reuter (8 V)

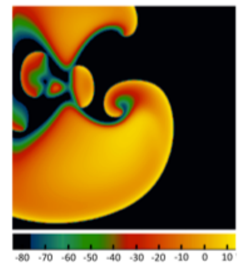

Ten-Tusscher-Panfilov (19V)

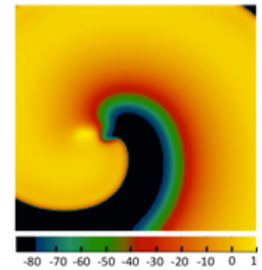

Iyer (65 V)

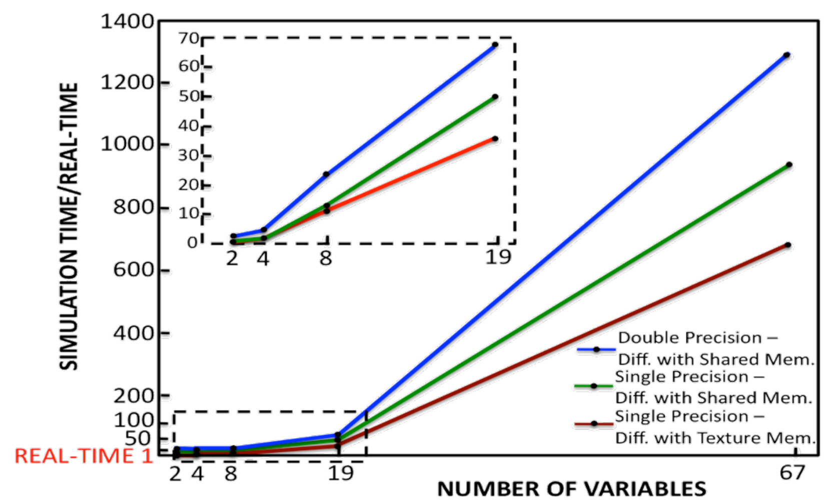

Zoo of Spirals Computed by Students at CMACS Seminar

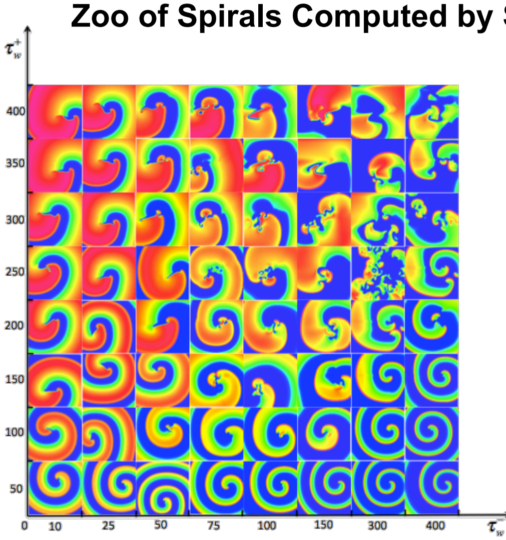

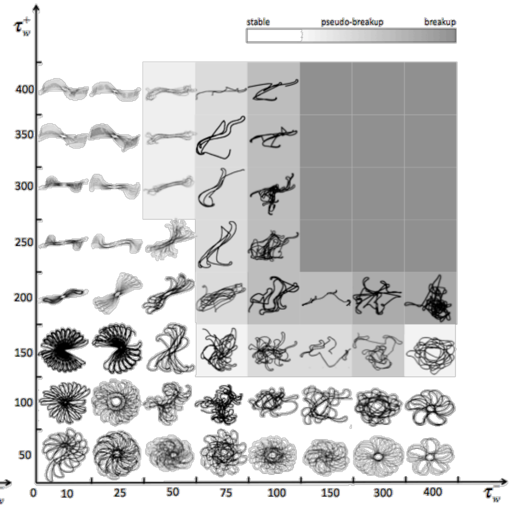

These results appeared this year in

CMSB 2011, pages 103-110, ACM, 2011

Advances in Physiology Education 35: 1-11, 2011

Analysis: WebGL Interactive Simulation and 3D-Models Simulation

Web Graphics Language (Fenton-Karma 2V)

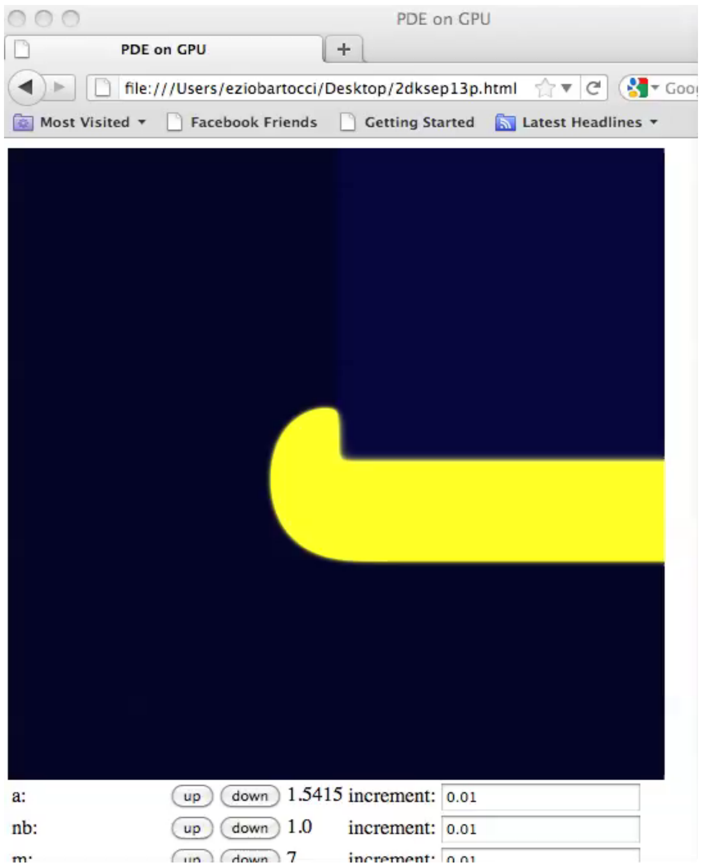

Runs in your Browser and uses your GPU

3D Model of a Rabbit Heart (Fenton-Karma 3V Model)

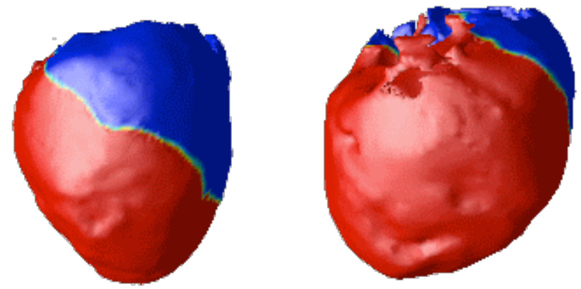

3D Model of a Pig Heart (Fenton-Karma 3V Model)

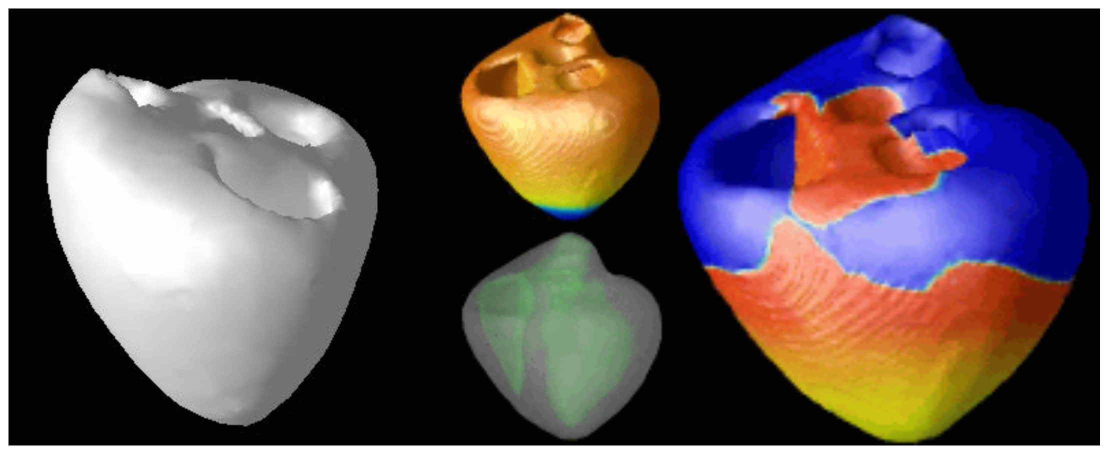

These results are work in progress

Analysis: Parameter-Range Inference for Unexcitability with Rovergene

Spiral Wave Induced by Unexcitable Myocytes

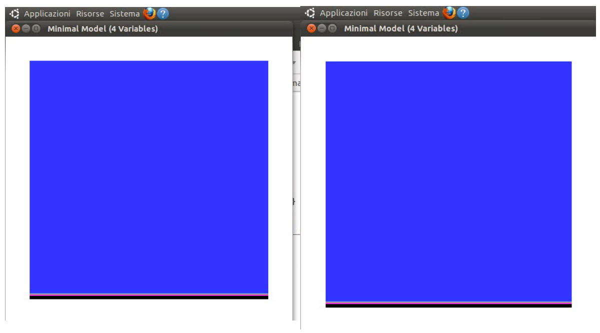

State-Space Partition

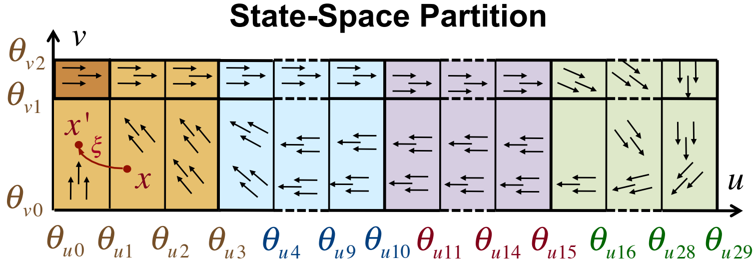

Kripke Structure for Fixed Parameters

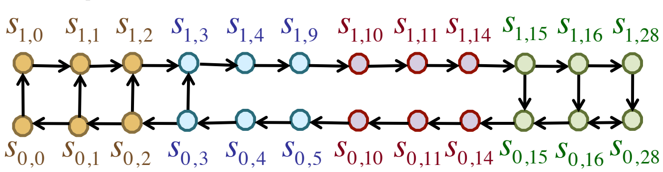

Computation of transitions:
By examining corner flows

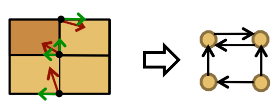

Genetic regulatory network with Parameters *κ,γ*

$$\dot{x}_i = f_i(x,p) = \sum_{j \in P_i} \kappa_{ij} r_{ij}(x) - \sum_{j \in D_i} \gamma_{ij} r_{ij}(x) x_i$$

Ramp Product r_{ij}

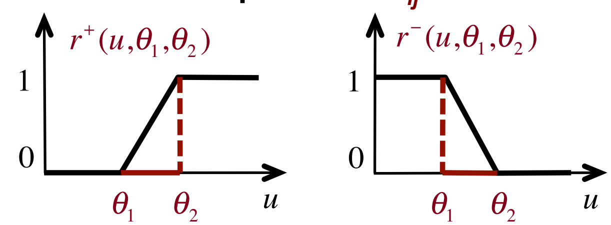

Parameter-Space Partition

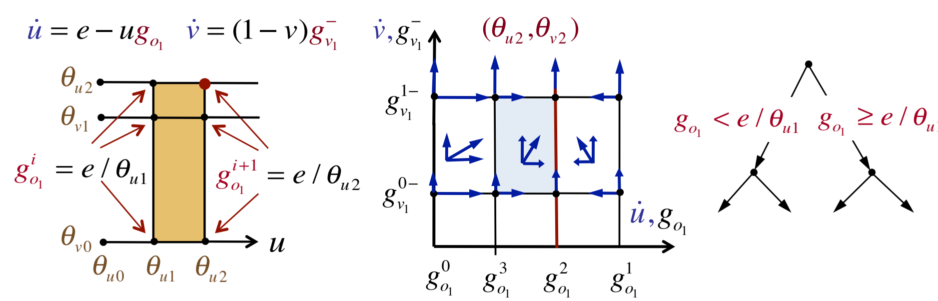

Property to Check and Uncertain Parameters

$$G(u < \theta_v),\ g_{o_1} \in [0,180],\ g_{o_2} \in [0,10],\ g_{o_2} \in [0,10],\ g_{o_2} \in [0,10]$$

Analysis: Parameter-Range Inference for Unexcitability with Rovergene

Parameter-Range Identification Results

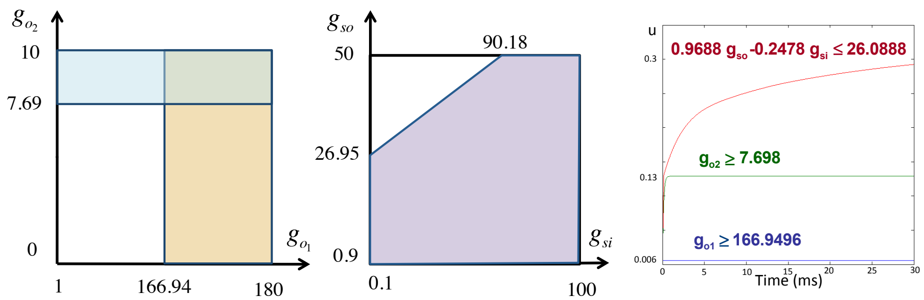

State-Space Partition

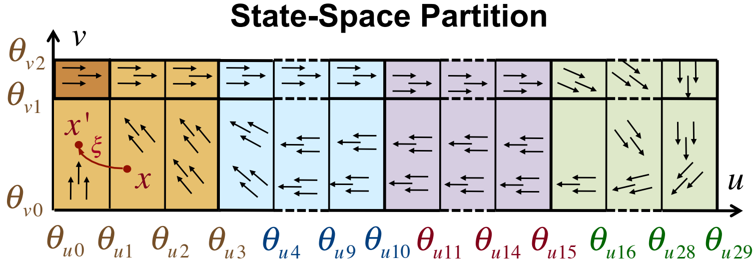

Kripke Structure for Fixed Parameters

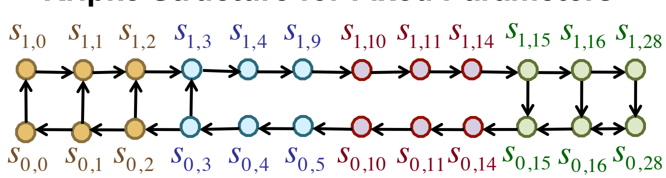

Computation of transitions:
By examining corner flows

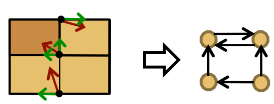

Genetic regulatory network with Parameters *κ,γ*

$$\dot{x}_i = f_i(x,p) = \sum_{j\in P_i} \kappa_{ij} r_{ij}(x) - \sum_{j\in D_i} \gamma_{ij} r_{ij}(x) x_i$$

Ramp Product r_{ij}

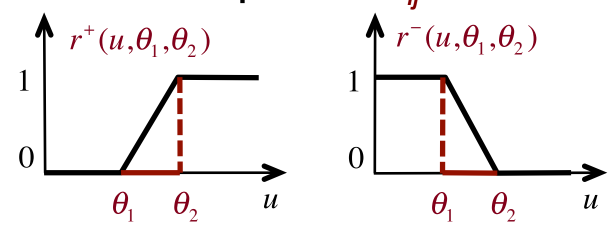

Parameter-Space Partition

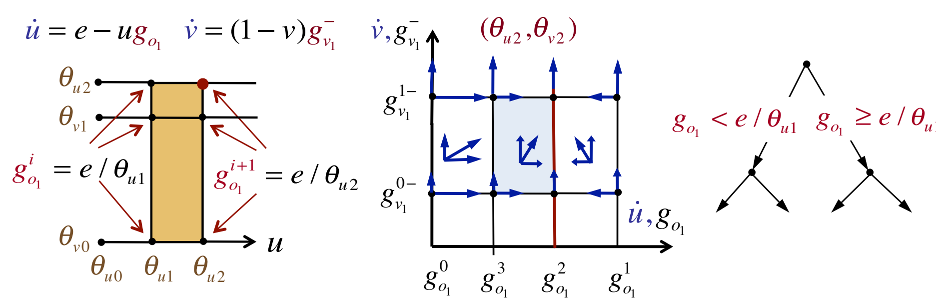

1st automatic parameter-range identification of abnormal behavior

These results appeared this year in CAV 2011, LNCS 6806, pp. 396-411, 2011.

Analysis: Parameter-Range Inference with Time-dependence in SpaceRover

Linear Hybrid Automaton of a Kripke Structure

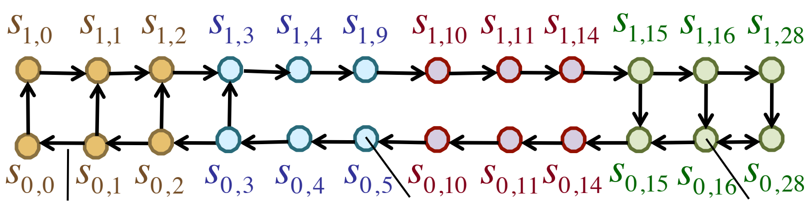

guard: face | **invariant:** all faces | **flow:** as below

Computation of Flows

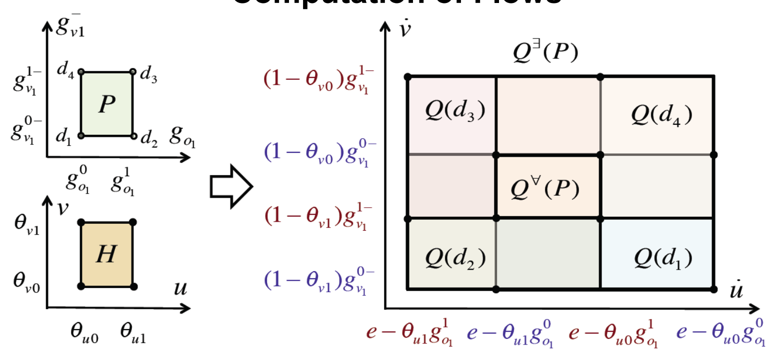

Summary of simulation relations

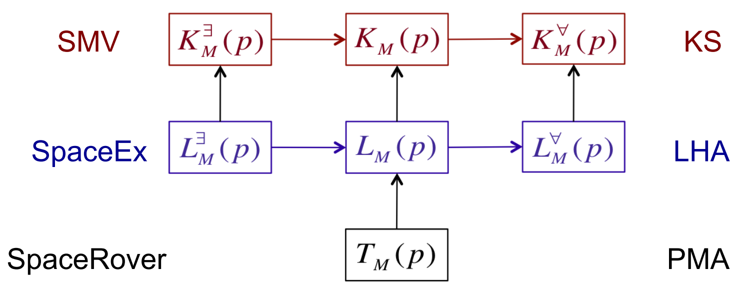

SpaceRover Search Algorithm

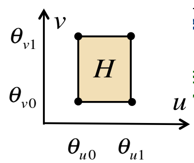

...t SpaceRover(M,φ,P)

...system $M=(f,\Pi)$, formula φ over Π, rectangular set P of uncertain parameters

...' of valid parameter sets

P,V,g,Ψ

3: ComputeParamConstraints()
4: TestParamSet(Ψ,ε)
5: return V
}

ComputeParamConstraints(f,Π,P)
{
// output: List of parameter constraints Ψ
// output: Function g with $g(H_1,H_2)=\cup_{c\in F}Q(c)$ where H_1,H_2 are adjacent hyper-rectangles with
// separating face F, c are its corners, and $Q(c)\doteq f(c,p)>0$ on direction $H_1\to H_2$
1: $\Psi := \varnothing$; $g := \varnothing$
2: forall (hyper-rectangles H in f and c in C_H and i in 1:n) $\Psi := \Psi\cup f_i(c,p)$
3: Ψ := RemoveRepeatedElementsAndSort(Ψ)
4: forall (adjacent rectangles H_1,H_2 in f) $g(H_1,H_2) := \cup_{c\in F} f(c,p)>0$ on direction $H_1\to H_2$
5: return (Ψ,g)
}

TestParamSet(Ψ,l)
{
// input: List of current parameter constraints l
// input: List of parameter constraints Ψ
// output: list V of valid parameter sets
1: Q := Polytope(l)
2: ($K_M^{\exists}(Q)$, $L_M^{\exists}(Q)$, $L_M^{\exists}(Q)$) := ConstructTransitionSystems(Q)
3: if (SMV($K_M^{\exists}(Q)$, φ)) $V := V\cup Q$; return
4: elseif (SpaceEx($L_M^{\exists}(Q)$, φ)) $V := V\cup Q$; return
5: elseif ($\neg$SpaceEx($L_M^{\forall}(Q)$, φ)) return
6: else { c := first(Ψ); Ψ := rest(Ψ); TestParamSet(Ψ, $l:\neg c$); TestParamSet(Ψ, $l:c$) } endif
}

Analysis: Parameter-Range Inference with Time-dependence in SpaceRover

Linear Hybrid Automaton of a Kripke Structure

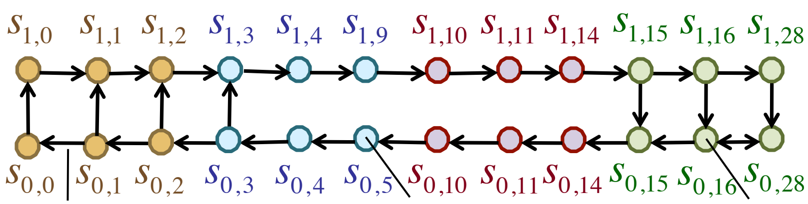

guard: face | **invariant:** all faces | **flow:** as below

Computation of Flows

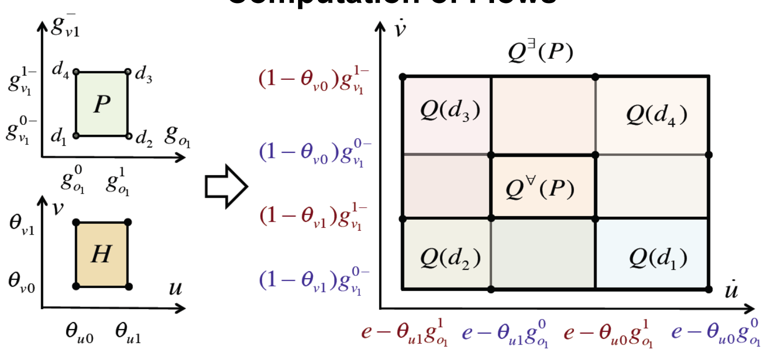

Summary of simulation relations

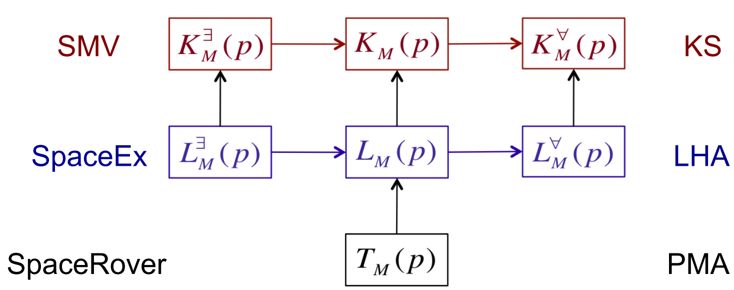

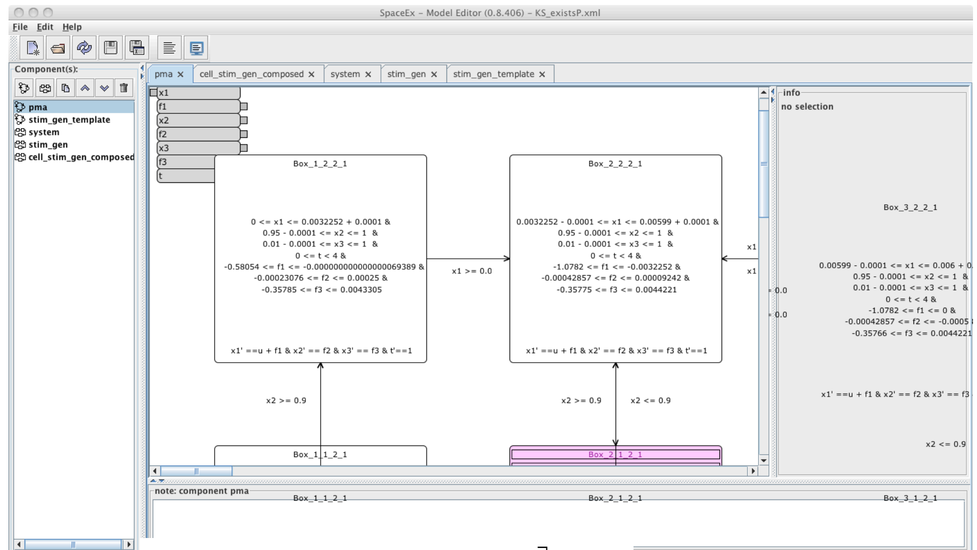

SpaceEx Execution for $L^{\exists}_M(P)$

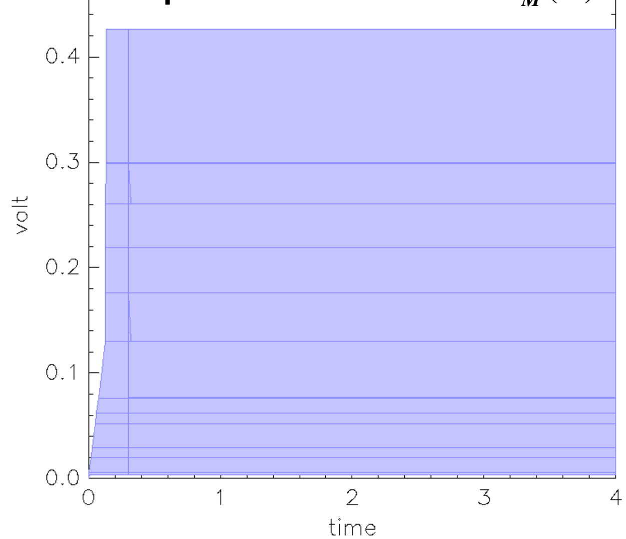

These results
Are work in progress

Analysis: Spiral Classification Algorithm for Isotropic Diffusion

For what parameter ranges does MHA accurately reproduce the cardiac disorder ?

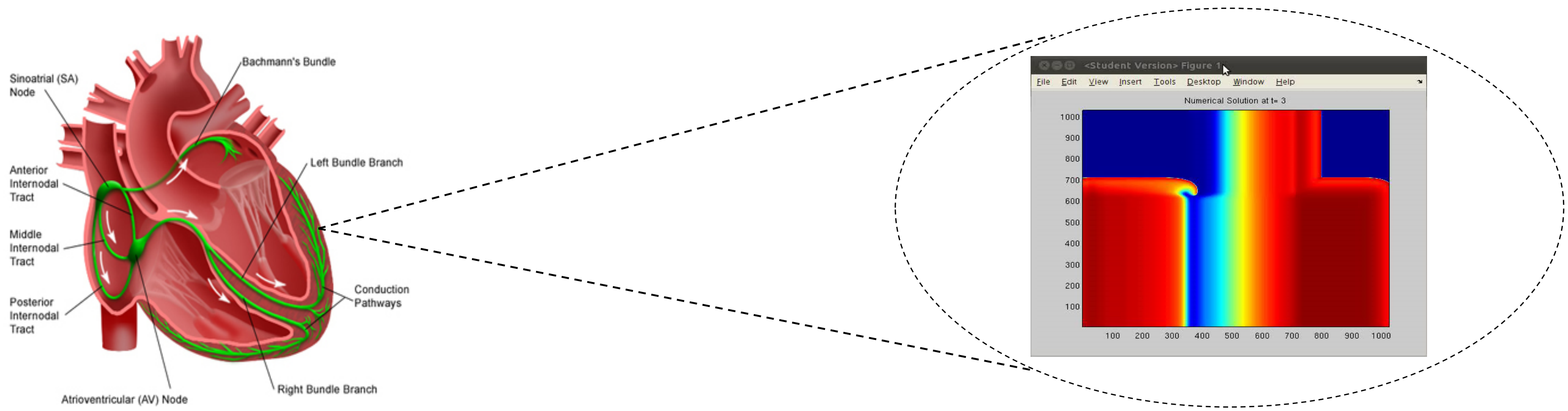

Setting: MHA simulation on 1024X1024 grid under isotropic diffusion

Parameter Identification = Principled Parameter-space partitioning + Bad behavior detection Using wave curvature – Spiral Classification Algorithm (SCA)

Why wave curvature: $\theta = \theta_0 - \frac{D}{r}$

θ = curved wave propagation velocity
θ_0 = flat wave propagation velocity
D = constant based on properties of medium
r = radius of curvature

Wave break (fibrillation) at critical radius: $r_c = \frac{D}{\theta_0}$

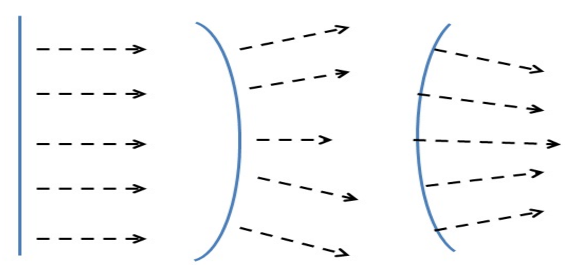

$\theta = \theta_0$ $\theta < \theta_0$ $\theta > \theta_0$

Analysis: Spiral Classification Algorithm for Isotropic Diffusion

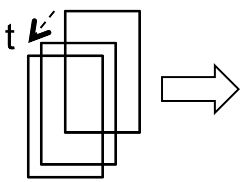

Parallel Isopotential Reconstruction Algorithm (PIRA) → **Weighted Average based Bézier Curve Fitting** → **Symbolic Curvature Evaluation**

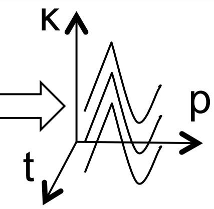

Simulation results

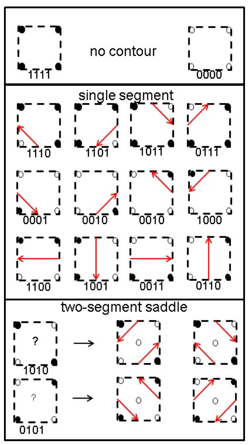

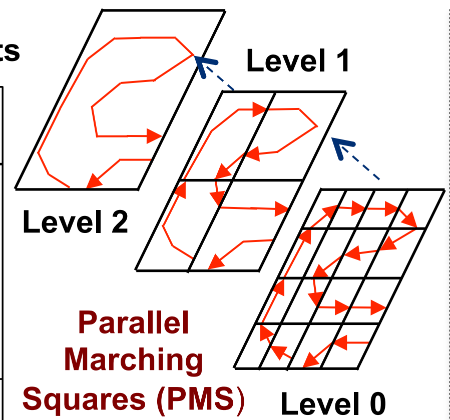

Parallel Marching Squares (PMS)

Implemented on NVIDIA GPU: 644X speed-up vs. Matlab's recursive contour

$$X_j(t) = (1-t)^3 P_j^0 + 3t(1-t)^2 P_j^1 + 3t^2(1-t) P_j^2 + t^3 P_j^3$$

$$Y_j(t) = (1-t)^3 Q_j^0 + 3t(1-t)^2 Q_j^1 + 3t^2(1-t) Q_j^2 + t^3 Q_j^3$$

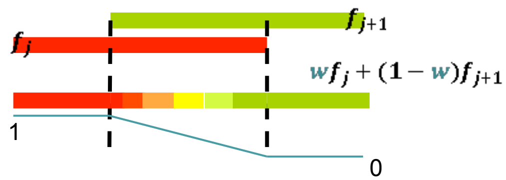

Uniform length strips.

Least squares fitting.

C2 continuity: weighted-average-based smoothing

$$\kappa_j(t) = \frac{|r_j'(t) \times r_j''(t)|}{|r_j'(t)|^3}$$

$$r_j(t) = [X_j(t), Y_j(t)]$$

Curvature based signatures of arrhythmia

Symbolic functions

Can be evaluated at any spatial resolution

These results appeared this year in CMSB'11, pp. 120-127, ACM, 2011

Wavelet-based analysis and Time-frequency logic development Is work in progress

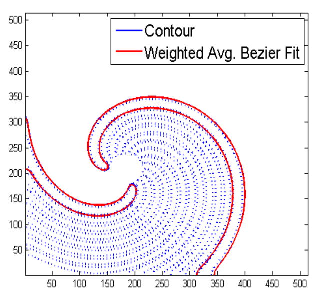

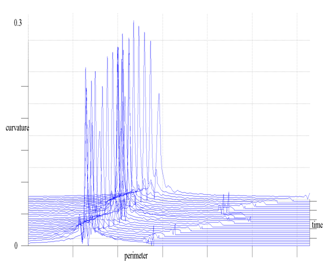

CASE STUDY: Spiral re-entry with circular core.

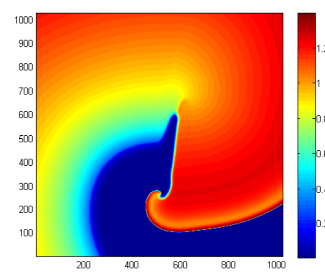

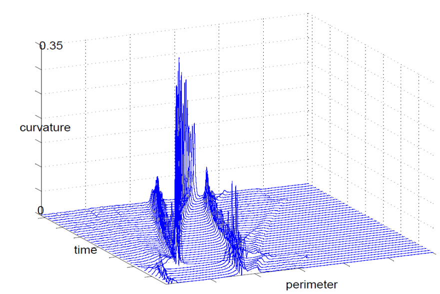

CASE STUDY: Spiral reentry with linear core.

Analysis: GPU / Multi-core Model Checking

Optimizing Spin software model checker with GPU / Multi-cores

- Exploring and comparing OpenCL/CUDA technologies
- Developing GPU-based efficient hashing algorithms
- Developing a GPU-based State Exploration Engine
- Developing a GPU-based State Verification Engine

Optimizing SAT/SMT solvers with GPU / Multi-cores

- SMT solvers seem most promising

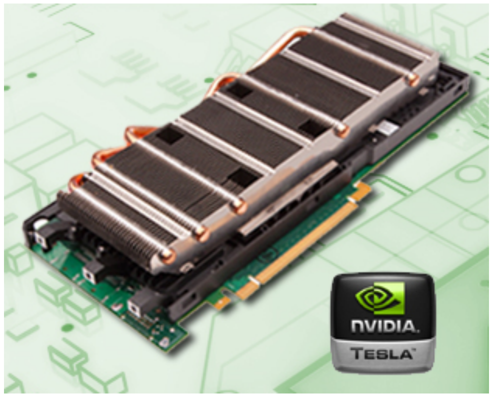

This is work in progress

Control: Termination of Arrhythmias with Low Energy Defibrillation

In the heart, fibrillation is one of the most dangerous arrhythmias, is produced by fast reentrant (spiral) waves of electrical activity and can occur in the atria or ventricles

Atria: Atrial fibrillation (AF) is the most common tachyarrhythmia worldwide.

Ventricle: Ventricular fibrillation (VF) is the leading cause of death in the US.

Based in concepts of complex systems and nonlinear dynamics we have developed a method to terminate reentrant arrhythmias in both atria and ventricles uses much lower energies compared to standard defibrillators (up to 360J [1000V, 30-45 Amps] which not only are very painful, they can damage cardiac tissue)

Termination by synchronization using multiple low energy shocks rather than one big one.

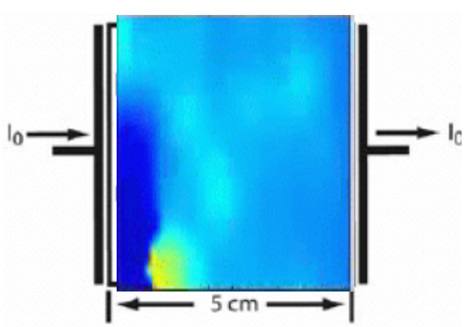

Computer simulation (proof of principle)

In vivo atrial fibrillation termination

1 Shock

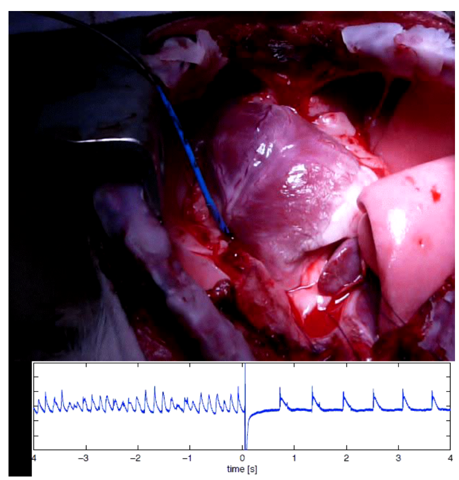

5 Low Energy Shocks

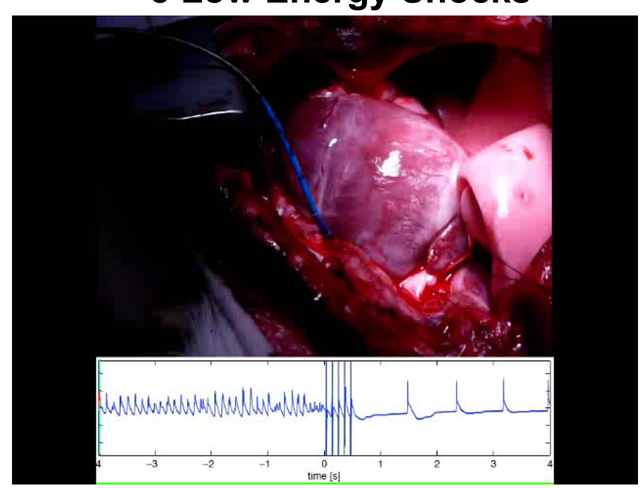

Defibrillation with 90% energy reduction

Control: Termination of Arrhythmias with Low Energy Defibrillation

Low Energy Defibrillation (LEAP) tested for Canine Hearts

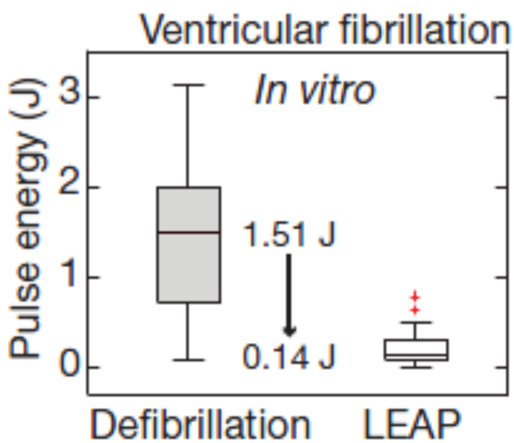

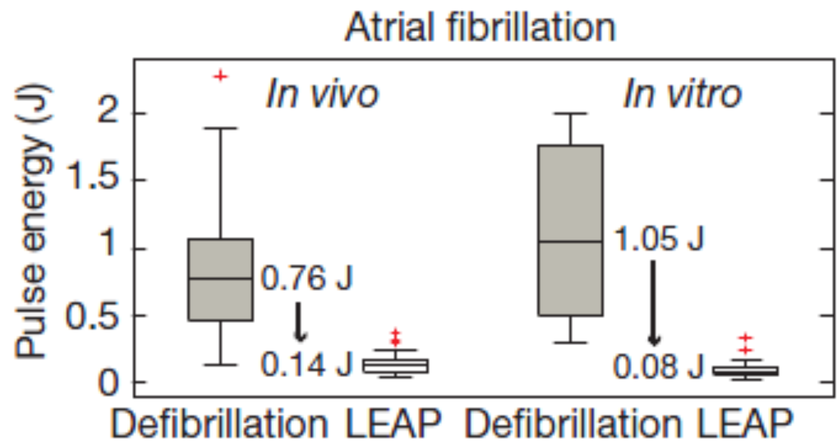

For Both AF and VF we have found successful defibrillation with LEAP using about10% of the energy required by the standard 1 shock defibrillation protocol

Furthermore, using high resolution mCT We obtained detail vessel distribution of the heart and found a scaling law which was used to obtain a theory that explains the mechanism behind LEAP.

These results appeared this year in Nature Jul 13;475(7355):235-9; 2011

Control: Model Repair for Discrete-Time Markov Chains

Knuth & Yao fair die problem

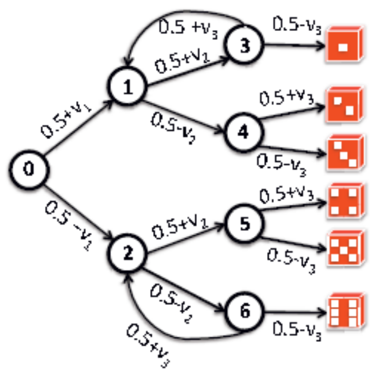

Property to Satisfy

$$\mathcal{P}_{\leq 1/8} F[die = 1]$$

Optimization Constraint to Satisfy and Transfer Function

$$\min\ w_1 v_1^2 + w_2 v_2^2 + w_3 v_3^2$$

$$\frac{8v_1v_2v_3 - 4(v_2v_1 - v_2v_3 - v_1v_3) - 2(v_1 + v_2 - v_3) - 1}{8v_2v_3 + 4v_2 + 4v_3 - 6} - \frac{1}{8} \leq 0$$

$$\forall i \in \{1, \cdots, 3\}, -0.5 < v_i < 0.5$$

When is Model Repair not feasible?

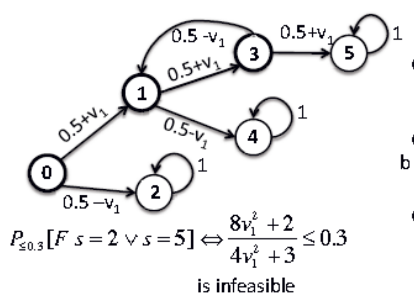

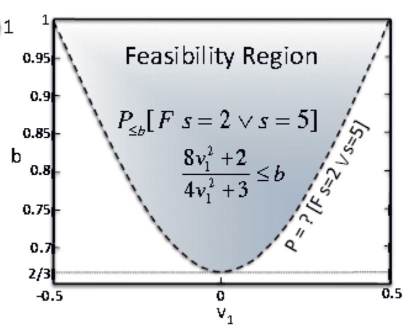

Solution found for $w = [1,1,1]$

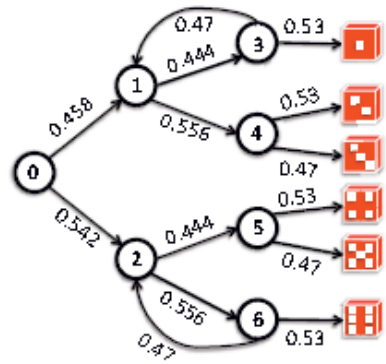

Solution found for $w = [10,5,1]$

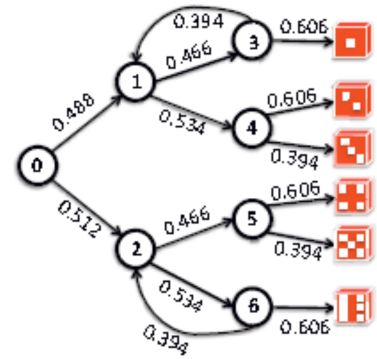

These results appeared this year in TACAS 2011, LNCS 6605, pp. 326–340, 2011